Green synthesis and surface functionalization of zinc oxide nanoparticles with glutamine/pluronic F127 for enhanced antimicrobial activity

Nguyen Ngoc Son*

Institute of Materials, Biology and Environment, Academy of Military Science and Technology, 17 Hoang Sam, Nghia Do, Hanoi, Vietnam.
*Corresponding author: sonorgc88@gmail.com.
Received 22 May 2026; Revised 09 Jul. 2026; Accepted 13 Jul. 2026; Published 25 Aug. 2026.
DOI: https://doi.org/10.54939/1859-1043.j.mst.113.2026.66-72

ABSTRACT

This study presents the stepwise surface functionalization of zinc oxide nanoparticles (ZnO NPs) with glutamine (Gln) and Pluronic F127 block copolymer to develop a highly stable, anti-agglomeration biocidal nanoplatform (ZnO@Gln-F127). Comprehensive characterization via FTIR, TEM, and EDX confirmed the sequential modification, revealing a multi-core and single-shell architecture where Gln firmly coordinates to ZnO and anchors the thick F127 polymer matrix via multiple hydrogen bonds. Thermogravimetric analysis quantitatively verified this structural evolution, recording a significant 41.31% organic mass loss. Overcoming the inherent agglomeration of pristine ZnO, the ZnO@Gln-F127 system exhibited superior, concentration-dependent antimicrobial efficacy against Gram-positive Bacillus subtilis and yeast Saccharomyces cerevisiae. The amphiphilic F127 shell provided exceptional colloidal stability through steric hindrance and enhanced microbial interactions, achieving complete eradication of both strains at 1.0 mg/mL. Ultimately, these findings highlight the immense potential of this hierarchical nanostructure for advanced biomedical applications.

Keywords: ZnO nanoparticles; Glutamine; Pluronic F127; Hierarchical modification; Antimicrobial activity.

1. INTRODUCTION

Zinc oxide (ZnO) nanomaterials are extensively studied in the biomedical field, combining photocatalytic activity and biocompatibility for applications ranging from tumor inhibition [1-4] to broad-spectrum antimicrobial treatments via reactive oxygen species (ROS) generation and Zn^{2+} diffusion [5]. However, pristine ZnO's high surface energy causes severe thermodynamic agglomeration in physiological media, drastically reducing its biocidal efficacy [5]. Surface functionalization using amino acids is essential to overcome this [6, 7] significantly enhancing biomedical performance [8]. Glutamine (Gln) serves as an effective primer; its α-amino and α-carboxylate groups coordinate with Zn^{2+}, while the polar amide side chain creates a hydrophilic interface [9]. To ensure long-term stability, Pluronic F127 (PEO-PPO-PEO) is anchored onto this layer, preserving the core's activity [10] and optimizing antimicrobial kinetics [11]. The hydrophobic PPO block interacts with Gln, while hydrophilic PEO chains provide robust steric hindrance against nonspecific protein adsorption [12, 13]. Unlike previous studies focusing on targeted chemotherapeutic drug delivery [14, 15]. this study pioneers the hierarchical modification (ZnO → ZnO@Gln → ZnO@Gln-F127) strictly to optimize broad-spectrum biocidal performance. Importantly, these findings aim to provide a theoretical foundation for practical military technologies, such as developing antibacterial wound dressings for field medicine and bio-fouling resistant coatings for military equipment.

2. MATERIALS AND METHODS

2.1. Materials

The precursors utilized for the synthesis and surface modification of the nanoparticles included zinc acetate dihydrate ($Zn(CH_3COO)_2.2H_2O$, ≥ 98%, Sigma-Aldrich), sodium hydroxide (NaOH,

≥99%, Merck), L-glutamine ($C5H_{10}N_2O_3$, ≥99%, Sigma-Aldrich), and Pluronic F127 block copolymer (Mw ~12,600, Sigma-Aldrich). All chemicals were of analytical grade and used directly without further purification. Deionized water and absolute ethanol were employed as solvents throughout the experimental, purification, and washing procedures. For the bioactivity assays, the model microbial strains utilized included the Gram-positive bacterium *Bacillus subtilis* and the yeast *Saccharomyces cerevisiae*.

2.2. Methods

2.2.1. Ultrasound-assisted green synthesis of ZnO nanoparticles

Pristine ZnO nanoparticles were fabricated via an ultrasound-assisted green synthesis utilizing guava (Psidium guajava) leaf extract, thereby eliminating inorganic alkaline agents. The aqueous extract, prepared by heating 5 g of dried leaf powder in 100 mL of double-distilled water (80 °C, 60 min) and filtering, provided polyphenolic and flavonoid compounds that functioned dually as Zn^{2+} chelating and capping agents [5, 10]. Subsequently, 50 mL of 0.1 M $Zn(CH_3COO)_2 \cdot 2H_2O$ was directly mixed with 50 mL of the extract and sonicated (40 kHz) at 60 °C for 2 hours. Acoustic cavitation facilitated simultaneous nucleation, significantly enhancing colloidal homogeneity and restricting agglomeration. The resulting suspension was centrifuged (10,000 rpm, 10 min), washed sequentially with double-distilled water and absolute ethanol, and dried at 80 °C for 12 hours. Finally, calcination at 600 °C for 2 hours thoroughly decomposed the residual bio-organic framework and established the characteristic wurtzite ZnO cores for subsequent hierarchical functionalization.

2.2.2. Hierarchical surface modification of ZnO

First, 200 mg of pristine ZnO was dispersed in 100 mL of glutamine solution (5 mg/mL, pH 6.0) via probe sonication and magnetically stirred for 24 hours at room temperature to form bidentate chelate complexes [8, 9]. The recovered ZnO@Gln product was washed and dried at 60 °C. Subsequently, 150 mg of ZnO@Gln was redispersed in 100 mL of Pluronic F127 solution (2 mg/mL) and stirred at 4 °C for 16 hours [10, 15] to facilitate non-covalent multi-point hydrogen bonding. The final ZnO@Gln-F127 nanoplatform was washed with cold water and lyophilized at –50 °C for 48 hours.

2.2.3. Material characterization

Chemical bonding and functional groups were identified utilizing Fourier-transform infrared (FTIR) spectroscopy (Tensor II, Bruker) operating in the 400–4000 cm^{-1} range with a 4 cm^{-1} resolution via the KBr pellet technique. Thermal degradation behavior and organic coating mass fractions were quantified through thermogravimetric analysis (TGA, LABSYS evo) under a nitrogen flow (50 mL/min), heating 5–10 mg samples from room temperature to 700 °C at a rate of 10 °C/min. Surface morphology and elemental composition were concurrently examined using a JEOL-JMS 6490 scanning electron microscope (SEM) coupled with an energy-dispersive X-ray (EDX) detector at an accelerating voltage of 15 kV, following Au/Pd sputter-coating. Furthermore, detailed microstructural evaluations and primary particle size determinations were conducted on a JEM 2100 transmission electron microscope (TEM) at 80–200 kV, with specimens prepared by drop-casting diluted nanoparticle suspensions onto carbon-coated copper grids.

2.2.4. Evaluation of antimicrobial activity

The microbial growth-inhibitory activity of the synthesized materials was quantitatively evaluated via the colony counting method in accordance with standard microbiological guidelines (CLSI). The tested model strains included the Gram-positive bacterium Bacillus subtilis and the yeast Saccharomyces cerevisiae. Microbial suspensions, cultured to a standard concentration of approximately 10^6 CFU/mL, were directly incubated with the ZnO, ZnO@Gln, and ZnO@Gln-F127 nanoparticles at concentrations of 0 mg/mL (serving as the negative control), 0.5 mg/mL,

and 1.0 mg/mL in a liquid medium at 37 °C. Following the incubation period, the samples were uniformly spread onto nutrient agar plates and incubated at 37 °C for an additional 24 hours. The antimicrobial efficacy was ultimately determined by observing and comparing the surviving colony density on the agar surface relative to the control sample.

3. RESULTS AND DISCUSSION

3.1. FTIR spectral analysis

FTIR spectra (Figure 1) confirm the sequential functionalization. Free Gln exhibits characteristic bands: ν(N–H) at 3275 cm^{-1}, Amide I ν(C=O) at 1702 cm^{-1}, and carboxylate stretches at 1493 and 1354 cm^{-1}[16]. In ZnO@Gln, the ν(N–H) shift to 3456 cm^{-1}, disappearance of the 2484 cm^{-1} band, and new ν(Zn–O)/ν(Zn–N) vibrations (400–650 cm^{-1}) indicate stable bidentate chelate ring formation via α-amino and α-carboxylate groups [17]. The unmodified Amide I band confirms the polar –$CONH_2$ side chain extends outward. The ZnO@Gln-F127 spectrum displays the F127 fingerprint: ν(C–H) at 2924 cm^{-1}, and triplet bands at 1272, 1103, and 951 cm^{-1} [12]. Crucially, shifts in the Amide I band and adjacent regions (1605/1406 cm^{-1}) demonstrate multi-point hydrogen bonding between Gln's outward-facing amide groups and F127's PEO ether oxygens, successfully tethering the stealth shell while preserving the ZnO core (ν(Zn–O) at 569 cm^{-1}).

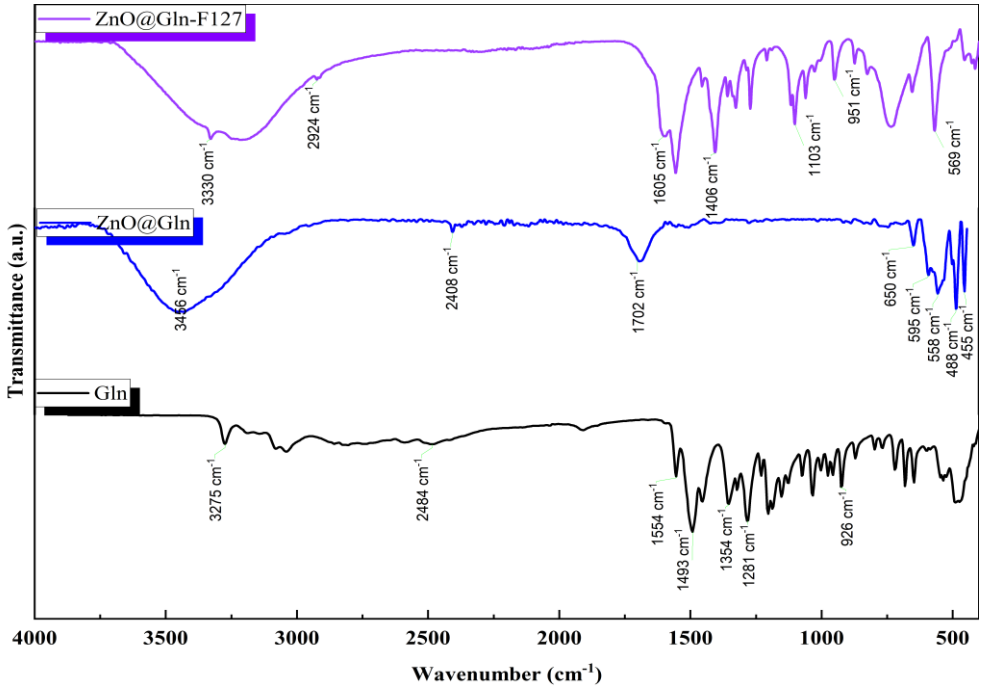

Figure 1. *FTIR spectra of free Gln, ZnO, ZnO@Gln, and ZnO@Gln-F127 nanoparticles.*

3.2. Surface morphology and microstructure analysis

Morphological and microstructural transformations following each functionalization step are directly evidenced by scanning and transmission electron microscopy (SEM and TEM) (Figure 2). Pristine ZnO nanoparticles exhibit quasi-spherical and polygonal wurtzite morphologies with primary sizes of 20–40 nm. However, their elevated surface energy drives severe hard agglomeration. Upon glutamine functionalization (ZnO@Gln), the inorganic core dimensions remain largely unchanged, but hard agglomerates are replaced by softer cluster architectures. TEM reveals less distinct inter-particle boundaries connected by a thin, low-contrast organic border, confirming glutamine's role as an effective intermolecular bridge. A profound

morphological transformation occurs in the hierarchically modified ZnO@Gln-F127 system. SEM observations show individual nanoparticles obscured within a continuous, porous polymer matrix. Decisively, TEM corroborates a multicore-shell architecture, wherein clusters of electron-dense ZnO cores are thoroughly encapsulated by a thick, amorphous, electron-transparent F127 polymer shell. This structural integration validates the modification mechanism: glutamine serves as a polar anchor, enabling the hydrophilic PEO chains of Pluronic F127 to intertwine into a massive polymeric stealth layer. Consequently, this robust shell provides exceptional steric hindrance, which is crucial for preventing nonspecific protein adsorption and secondary agglomeration in physiological environments.

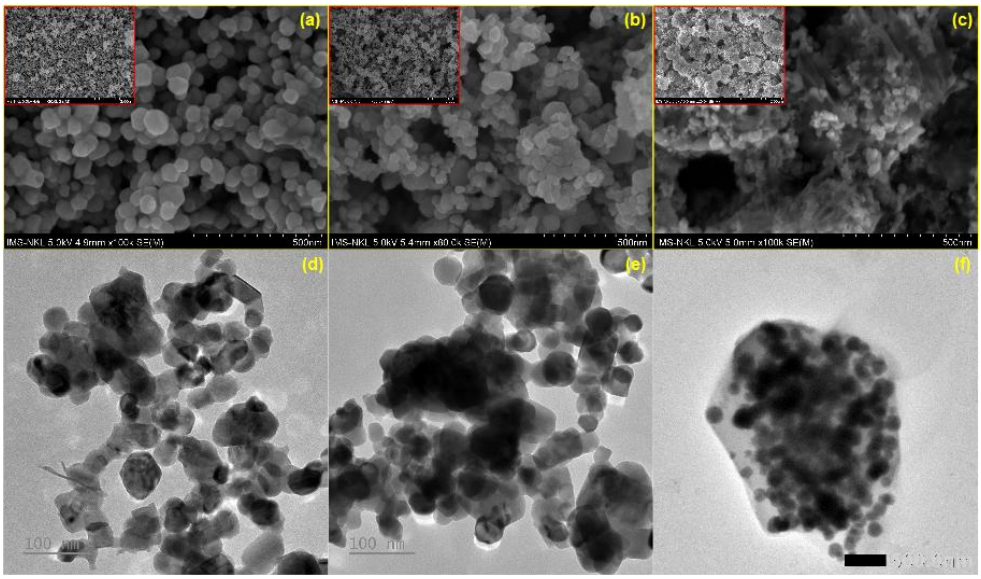

Figure 2. *Morphological and microstructural characterization: SEM micrographs of (a) pristine ZnO, (b) ZnO@Gln, and (c) ZnO@Gln-F127; TEM micrographs of (d) pristine ZnO, (e) ZnO@Gln, and (f) ZnO@Gln-F127.*

3.3. Elemental composition analysis

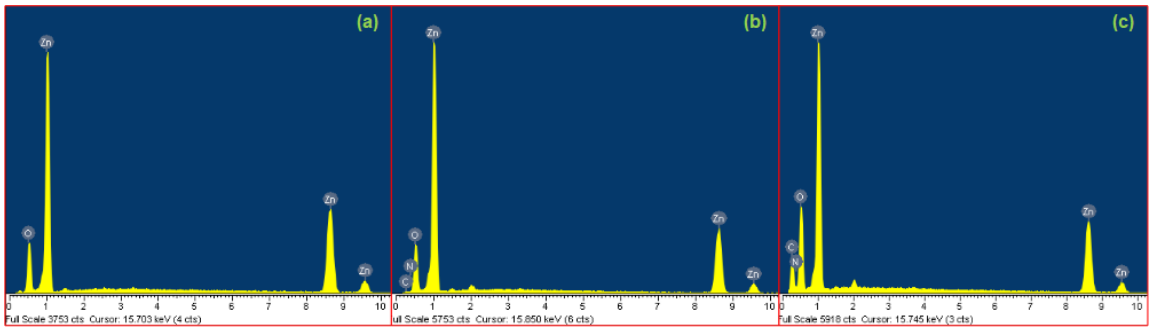

Figure 3. *Energy-dispersive X-ray (EDX) spectra of (a) pristine ZnO, (b) ZnO@Gln, and (c) ZnO@Gln-F127.*

EDX analysis (Figure 3, Table 1) quantitatively confirms the surface evolution. Following glutamine functionalization, ZnO@Gln exhibits distinct C (6.29 at%) and N (6.49 at%) signals. The profound structural transformation is manifested in the hierarchically modified ZnO@Gln-F127 sample, where carbon content drastically increases to 42.28 at% due to the massive PEO-PPO-PEO backbone. Concurrently, the core elements Zn and N experience a severe decline (to 12.44 at% and 2.28 at%, respectively), verifying a strong elemental shielding effect caused by the dense, overlying F127 polymer shell completely encapsulating the cores.

Table 1. *Surface elemental atomic percentages of ZnO, ZnO@Gln, and ZnO@Gln-F127 obtained from EDX results.*

Material	Zn (%at)	O (%at)	C (%at)	N (%at)
ZnO	48.80	51.20	–	–
ZnO@Gln	35.38	51.84	6.29	6.49
ZnO@Gln-F127	12.44	43.00	42.28	2.28

3.4. Thermogravimetric analysis (TGA)

TGA (Figure 4, Table 2) quantitatively verifies the organic coating mass. ZnO@Gln exhibits a 7.63% loss (desorbed water) and a 3.66% loss (500–650 °C) corresponding to Gln carbon backbone pyrolysis, confirming successful monolayer coordination. A profound transformation occurs in ZnO@Gln-F127, with a total mass loss reaching 41.31% (32.42% below 200 °C and 8.89% up to 450 °C). This substantial continuous decline reflects the degradation of F127's PEO/PPO segments and the evaporation of strongly retained water within the hydrophilic PEO network. This dramatic mass loss perfectly correlates with the carbon elemental leap observed in EDX (6.29 at% to 42.28 at%), providing robust quantitative evidence of complete nanoparticle encapsulation by the dense F127 shell.

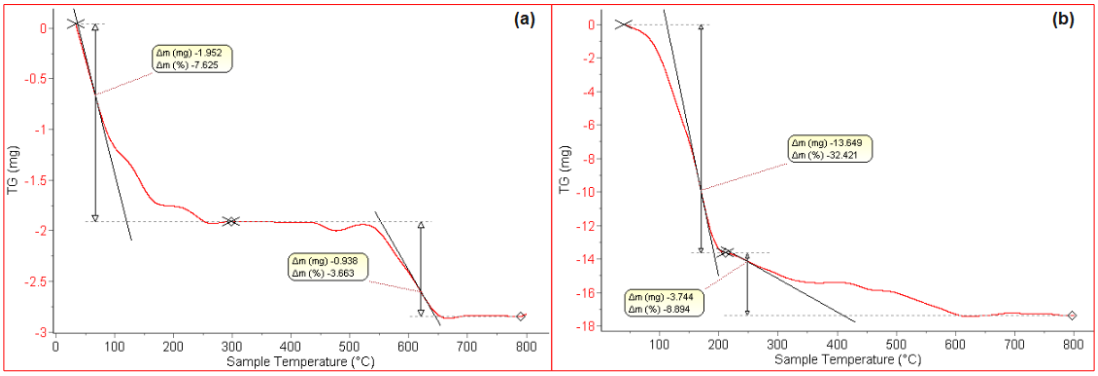

Figure 4. *Thermogravimetric analysis (TGA) curves of (a) ZnO@Gln and (b) ZnO@Gln-F127 nanoparticles.*

Table 2. *Quantitative mass loss percentages of surface-modified ZnO samples extracted from TGA thermograms at distinct temperature ranges.*

Materials	Weight loss < 200 °C (%)	Weight loss > 200 °C (%)	Total weight loss (%)	Residual weight at 800 °C (%)
ZnO@Gln	7.63	3.66	11.29	88.71
ZnO@Gln-F127	32.42	8.89	41.31	58.69

3.5. Antimicrobial activity

The colony counting method evaluated antimicrobial efficacy against *B. subtilis* and *S. cerevisiae* (Figure 5). Pristine ZnO exhibited limited inhibition at 0.5 mg/mL due to severe agglomeration, which diminishes the effective specific surface area.

Conversely, the hierarchically modified ZnO@Gln-F127 system demonstrated a quantum leap in performance, achieving near-complete inhibition at 0.5 mg/mL and absolute (100%) eradication at 1.0 mg/mL for both strains. This exceptional bioactivity stems from the core-shell architecture's synergistic effects. The bulky F127 shell provides robust steric hindrance, suppressing agglomeration and maximizing the effective contact area in physiological media. Furthermore, the amphiphilic F127 copolymer exhibits high affinity toward bacterial peptidoglycan and yeast cell walls, inducing severe membrane destabilization. Ultimately, this structural integration positions ZnO@Gln-F127 as a highly promising platform for advanced targeted antimicrobial applications.

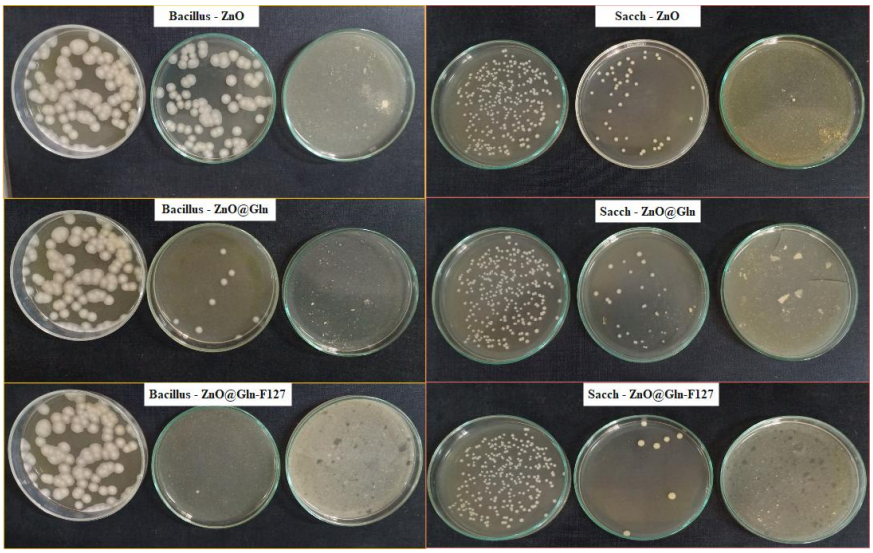

Figure 5. *Antimicrobial growth-inhibitory profiles showing the colony development of Bacillus subtilis and Saccharomyces cerevisiae treated with pristine ZnO, ZnO@Gln, and ZnO@Gln-F127 nanoparticles at concentrations of 0, 0.5, and 1.0 mg/mL.*

4. CONCLUSIONS

In summary, wurtzite ZnO nanoparticles synthesized via an ultrasound-assisted green method were successfully modified with glutamine and Pluronic F127 to construct a stable hierarchical multicore-shell architecture. Characterization verified that glutamine anchored onto the ZnO cores via bidentate chelation, facilitating the secondary encapsulation of a dense F127 polymer shell through multi-point hydrogen bonding with a quantified organic mass loss of 41.31%. By effectively suppressing thermodynamic agglomeration and resisting nonspecific protein adsorption in clinical environments, the engineered ZnO@Gln-F127 nanoplatform demonstrated exceptional antimicrobial efficacy, completely eradicating Bacillus subtilis and Saccharomyces cerevisiae at 1.0 mg/mL. These findings demonstrate the immense potential of this structurally integrated nanoplatform for advanced biomedical applications, specifically in developing antibacterial wound dressings for field medicine and bio-fouling resistant coatings for military equipment.

REFERENCES

[1]. Sirelkhatim, A., et al., "*Review on Zinc Oxide Nanoparticles: Antibacterial Activity and Toxicity Mechanism*", Nano-Micro Letters, Vol. 7, No. 3, pp. 219–242, (2015).
[2]. Djurišić, A.B., et al., "*ZnO nanostructures: growth, properties and applications*", Journal of Materials Chemistry, Vol. 22, No. 14, pp. 6526–6535, (2012).
[3]. Son, N.N., V.M. Thanh, and N.T. Huong, "*Anticancer Activities of Zinc Oxide Nanoparticles Synthesized Using Guava Leaf extract*", ChemistrySelect, Vol. 8, No. 45, pp. e202303214, (2023).
[4]. Bogdan, J., J. Pławińska-Czarnak, and J. Zarzyńska, "*Nanoparticles of Titanium and Zinc Oxides as Novel Agents in Tumor Treatment: a Review*", Nanoscale Research Letters, Vol. 12, No. 1, pp. 225, (2017).
[5]. Seil, J.T. and T.J. Webster, "*Antimicrobial applications of nanotechnology: methods and literature*", International Journal of Nanomedicine, Vol. 7, pp. 2767–81, (2012).
[6]. Ramani, M., et al., "*Amino acid-mediated synthesis of zinc oxide nanostructures and evaluation of their facet-dependent antimicrobial activity*", Colloids and Surfaces B: Biointerfaces, Vol. 117, pp. 233–239, (2014).
[7]. Stankic, S., et al., "*Pure and multi metal oxide nanoparticles: synthesis, antibacterial and cytotoxic properties*", Journal of Nanobiotechnology, Vol. 14, No. 1, pp. 73, (2016).
[8]. Huong, N.T., et al., "*Glutamic acid–coated zinc oxide nanoparticles: synthesis, characterization, and anticancer activity*", Journal of Nanoparticle Research, Vol. 27, No. 1, pp. 15, (2025).

[9]. Nejabatdoust, A., et al., "*Synthesis, Characterization and Functionalization of ZnO Nanoparticles by Glutamic Acid (Glu) and Conjugation of ZnO@Glu by Thiosemicarbazide and Its Synergistic Activity with Ciprofloxacin Against Multi-drug Resistant Staphylococcus aureus*", Journal of Cluster Science, Vol. 30, No. 2, pp. 329–336, (2019).
[10]. Nguyen Ngoc, S., T. Vu Minh, and H. Nguyen Thi, "*Pluronic F-127 modified ZnO nanoparticles: Green synthesis, surface modification, characterization and anticancer properties*", Journal of Military Science and Technology, Vol. 93, No. 93, pp. 91–98, (2024).
[11]. Huong, N.T., et al., "*Green synthesis and characterization of Pluronic coated Zinc nanoparticles from extracts of Tea leaf for antimicrobial activity*", Vietnam Journal of Catalysis and Adsorption, Vol. 13, No. 4, pp. 32–37, (2024).
[12]. Kabanov, A.V., E.V. Batrakova, and V.Y. Alakhov, "*Pluronic® block copolymers as novel polymer therapeutics for drug and gene delivery*", Journal of Controlled Release, Vol. 82, No. 2, pp. 189–212, (2002).
[13]. Nguyen Ngoc, S., T. Vu Minh, and H. Nguyen Thi, "*Synthesis and characterization of F127-Glu@ZnO nanogel material for cisplatin drug delivery application*", Journal of Military Science and Technology, Vol. FEE, pp. 237–242, (2024).
[14]. Son, N.N., V.M. Thanh, and N.T. Huong, "*Synthesis of F127-GA@ZnO nanogel as a cisplatin drug delivery pH-sensitive system*", RSC Advances, Vol. 14, No. 47, pp. 35005–35020, (2024).
[15]. Pitto-Barry, A. and N.P.E. Barry, "*Pluronic® block-copolymers in medicine: from chemical and biological versatility to rationalisation and clinical advances*", Polymer Chemistry, Vol. 5, No. 10, pp. 3291–3297, (2014).
[16]. Pawlukojć, A., et al., "*l-Cysteine: Neutron spectroscopy, Raman, IR and ab initio study*", Spectrochimica Acta Part A: Molecular and Biomolecular Spectroscopy, Vol. 61, No. 11, pp. 2474–2481, (2005).
[17]. Kanchana, U.S. and T.V. Mathew, "*Surface functionalization of ZnO nanoparticles with functionalized bovine serum albumin as a biocompatible photochemical and antimicrobial agent*", Surfaces and Interfaces, Vol. 24, pp. 101056, (2021).

TÓM TẮT

Tổng hợp, đặc trưng và đánh giá hoạt tính kháng khuẩn của hệ vật liệu nano ZnO biến tính bề mặt phân tầng bằng glutamine và pluronic F127

Nghiên cứu trình bày quá trình chức năng hóa bề mặt tuần tự hạt nano kẽm oxit (ZnO) bằng glutamine (Gln) và copolymer khối Pluronic F127 nhằm tạo nền tảng nano diệt khuẩn cực kỳ ổn định, chống kết tụ (ZnO@Gln-F127). Các phân tích FTIR, TEM và EDX xác nhận sự biến tính tuần tự này, hé lộ kiến trúc đa lõi - một vỏ, nơi Gln phối trí bền vững với ZnO và neo giữ ma trận F127 dày thông qua đa liên kết hydro. Phân tích nhiệt trọng lượng xác minh định lượng sự tiến hóa cấu trúc với mức tổn hao hữu cơ đáng kể 41,31%. Vượt qua nhược điểm kết tụ của ZnO nguyên bản, hệ ZnO@Gln-F127 thể hiện hiệu quả kháng vi sinh vật vượt trội, phụ thuộc nồng độ đối với vi khuẩn Gram dương Bacillus subtilis và nấm men Saccharomyces cerevisiae. Lớp vỏ F127 lưỡng phân tạo độ ổn định hệ keo xuất sắc nhờ án ngữ không gian và tăng cường tương tác vi sinh vật, tiêu diệt hoàn toàn cả hai chủng ở nồng độ 1,0 mg/mL. Những kết quả này khẳng định tiềm năng to lớn của cấu trúc nano phân tầng cho các ứng dụng y sinh tiên tiến.

Từ khoá: Hạt nano ZnO; Glutamine; Pluronic F127; Biến tính bề mặt phân tầng; Hoạt tính kháng khuẩn.